Sequence γ377−395(P2), but Not γ190−202(P1), Is the Binding Site for the α_MI-Domain of Integrin $\alpha_M\beta_2$ in the γC-Domain of Fibrinogen†

Tatiana P. Ugarova,*,‡ Valeryi K. Lishko,‡ Nataly P. Podolnikova,‡ Nobuo Okumura,§ Sergei M. Merkulov,‡,|| Valentin P. Yakubenko,‡ Vivien C. Yee,‡ Susan T. Lord,⊥ and Thomas A. Haas‡

Joseph J. Jacobs Center for Thrombosis and Vascular Biology, Department of Molecular Cardiology, Lerner Research Institute, Cleveland, Ohio 44195, Department of Biomedical Laboratory Sciences, School of Health Sciences, Shinshu University, Japan, and Department of Pathology and Laboratory Medicine, University of North Carolina, Chapel Hill, North Carolina 27599

Received January 13, 2003; Revised Manuscript Received April 30, 2003

ABSTRACT: The interaction between the leukocyte integrin $\alpha_M\beta_2$ (CD11b/CD18, Mac-1, CR3) and fibrinogen mediates the recruitment of phagocytes during the inflammatory response. Previous studies demonstrated that peptides P2 and P1, duplicating γ377−395 and γ190−202 sequences in the γC domain of fibrinogen, respectively, blocked the fibrinogen-binding function of $\alpha_M\beta_2$, implicating these sequences as possible binding sites for $\alpha_M\beta_2$. To determine the role of these sequences in integrin binding, recombinant wild-type and mutant γC domains were prepared, and their interactions with the α_MI-domain, a ligand recognition domain within $\alpha_M\beta_2$, were tested. Deletion of γ383−411 (P2-C) and γ377−411 produced γC mutants which were defective in binding to the α_MI-domain. In contrast, alanine mutations of several residues in P1 did not affect α_MI-domain binding, and simultaneous mutations in P1 and deletion of P2 did not decrease the binding function of γC further. Verifying the significance of P2, inserting P2-C and the entire P2 into the homologous position of the βC-domain of fibrinogen imparted the higher α_MI-domain binding ability to the chimeric proteins. To further define the molecular requirements for the P2-C activity, synthetic peptides derived from P2-C and a peptide array covering P2-C have been analyzed, and a minimal recognition motif was localized to γ^{390}NRLTIG^{395}. Confirming a critical role of this sequence, the cyclic peptide NRLTIG retained full activity inherent to P2-C, with Arg and Leu being important residues. Thus, these data demonstrate the essential role of the P2, but not P1, sequence for binding of γC by the α_MI-domain and suggest that the adhesive function of P2 depends on the minimal recognition motif NRLTIG.

The integrin $\alpha_M\beta_2$ (CD11b/CD18, Mac-1, CR3)[1] mediates multiple adhesive reactions of neutrophils and monocytes during the immune-inflammatory responses (*1*). The complexity of $\alpha_M\beta_2$ functions arises from its ability to recognize numerous ligands, and to date more than 30 proteins have been reported to bind $\alpha_M\beta_2$. The molecular features of ligands which allow their recognition by $\alpha_M\beta_2$ are currently unknown.

The interaction of $\alpha_M\beta_2$ with fibrinogen (Fg) has been directly implicated in leukocyte adhesive responses (reviewed in ref *2*), and recent characterization of $\alpha_M\beta_2$-deficient mice confirmed that Fg-dependent leukocyte adhesion was diminished in these animals (*3*). The $\alpha_M\beta_2$-binding site in Fg was localized to its D domain (*4*), which is structurally organized into two highly homologous domains, γC and βC, formed by ∼30 kD carboxyl-terminal portions of the γ- and β-chains, respectively (*5*). Previous studies have demonstrated that the binding site for $\alpha_M\beta_2$ resides in the γC-domain (*6*). On the basis of studies with synthetic peptides, two sequences, ^{190}GWTWFQKRLDGSV^{202} (designated P1) and ^{377}YKSMKKTTMKIIPFNRLTIG^{395} (designated P2), within γC have been proposed as essential in recognition of the $\alpha_M\beta_2$ (7;8). Both P1 and P2 peptides inhibit adhesion of the $\alpha_M\beta_2$-expressing cells, directly support $\alpha_M\beta_2$-mediated adhesion, and are also able to promote migration of the $\alpha_M\beta_2$-expressing cells (*9*). Since on a molar basis P2 was ∼10-fold more potent than P1 in inhibiting adhesion of the $\alpha_M\beta_2$-expressing cells (*8*), the P2 sequence has been implicated as the major binding site for the $\alpha_M\beta_2$. Analyses of the adhesion-promoting and inhibitory activities of overlapping peptides spanning P2 showed that although its amino-terminal portion (γ377−386) was active, it was the carboxyl-terminal part, ^{383}TMKIIPFNRLTIG^{395}, designated P2-C, that

† This work was supported by NIH Grants HL 63199 and HL 17964 and by Biogen, Inc. and was done during the tenure of an Established Investigatorship of the American Heart Association (T.P.U.).

* To whom correspondence should be addressed at the Cleveland Clinic, Mail Code NB 50. E-mail: ugarovt@ccf.org. Tel: (216) 445-8209. FAX: (216) 445-8204.

‡ Lerner Research Institute.

§ Shinshu University.

|| Present address: Department of Medicine, Case Western Reserve University.

⊥ University of North Carolina.

[1] Abbreviations: Fg, human fibrinogen; γC and βC, globular COOH-terminal domains of the γ- and β-chains of Fg; I-domain, a region of ∼200 amino acid residues "inserted" in the α_M subunit of integrin $\alpha_M\beta_2$; P2, P2-C, and P1, the γC-domain sequences corresponding to γ377−395, γ383−395, and γ190−202; HEK 293 cells, human embryonic kidney cells; GST, glutathione S-transferase; ICAM-1, intercellular cell adhesion molecule 1, BSA, bovine serum albumin; HBSS, Hanks balanced salt solution; PVP, poly(vinylpyrrolidone); PVA, poly(vinyl alcohol); TBS, Tris-buffered saline; mAb, monoclonal antibody.

10.1021/bi034057k CCC: $25.00
Published on Web 07/16/2003

Table 1: Inhibition of Adhesion of the $\alpha_M\beta_2$-Expressing Cells by P2 and P2-C-Derived Peptides[a]

name	position in the γC-domain	sequence	IC_{50}, μM
P2	377−395	YSMKKTTMKIIPFNRLTIG-OH	41 ± 8
P2-C-OH	383−395	TMKIIPFNRLTIG-OH	42 ± 10
P2-C-NH_2	383−395	TMKIIPFNRLTIG-NH_2	41 ± 10
	388−395	PFNRLTIG-OH	245 ± 80
	388−395	PFNRLTIG-NH_2	180 ± 65
	388−395(L392D)	PFNRDTIG-NH_2	>2000
	390−395	NRLTIG-OH	1160 ± 120
	390−395	NRLTIG-NH_2	1750 ± 240
	388−393	PFNRLT-OH	1600 ± 190
	390(R391E)−395	NELTIG-NH_2	≫2000
cyclic	390−395	C−NRLTIG-C− NH_2	70 ± 20
P2-CE	383−395 (K385E, R391E)	TMEIIPFNELTIG-NH_2	240 ± 40

[a] Calcein-labeled cells were incubated with increasing concentrations of P2, P2-C, or P2-C-derived peptides, and aliquots containing 2.5×10^4 cells were added to microtiter plates coated with 2 μg/mL D_{100}. After 30 min at 37 °C, nonadherent cells were removed by three washes with PBS. Fluorescence of adherent cells was measured in a fluorescent plate reader and converted to cell numbers. Results are expressed as a peptide concentration required to attain 50% inhibition (IC_{50}) and are the mean ± SE values from 3−8 individual experiments done in triplicate.

was primarily responsible for the inhibitory activity of P2 (8). Within $\alpha_M\beta_2$, the α_MI-domain has been demonstrated to be sufficient for full adhesiveness of $\alpha_M\beta_2$ to Fg (*10*). Accordingly, the binding site for the P2-C peptide was localized to the segment Lys^{245}−Arg^{261} within the α_MI-domain (*11*). Yet, despite a wealth of information about Fg peptides and their functional responses, it is unknown whether P2 and P1 sequences function as the binding sites for $\alpha_M\beta_2$ within the γC-domain.

To gain an understanding of the molecular basis for recognition of Fg by $\alpha_M\beta_2$, γC domain mutants with progressive deletions in the P2 sequence alone or in combination with mutations in the P1 sequence have been prepared. The γC-domains with truncated P2-C and P2 were equally deficient in their ability to bind the α_MI-domain. In contrast, mutating the P1 site alone, or simultaneously with P2, did not result in a further loss of the binding activity. Verifying the role of P2 in the α_MI-domain binding, inserting the P2-C and P2 sequences into the related Fg domain, βC, imparted the higher binding ability to the βC/γC chimera. In addition, to define the basis for the P2-C activity, structure−function analyses of the P2-C peptide have been performed, and a critical $\alpha_M\beta_2$ recognition motif was identified. We anticipate that defining the binding site for Fg may help to unravel the principles that govern multiligand recognition by $\alpha_M\beta_2$.

MATERIALS AND METHODS

Proteins, Peptides, and Antibodies. The fragment D_{100} (M_r 100 kD) was prepared by digestion of human Fg with plasmin as described (*12*). The expression, purification and characterization of the α_MI-domain as a fusion protein with GST have been previously described (*11*). To cleave the α_MI-domain from the fusion part, 15 units of human thrombin (Enzyme Research Laboratories, South Bend, IN) was added to 3.0 mL of glutathione-agarose beads bound with GST-I-domain (a molar ratio of thrombin:α_MI-domain 1:∼1000). The mixture was incubated for 1 h at 22 °C, and 1 mM phenylmethylsulfonyl fluoride was then added to inactivate thrombin. In selected experiments, the α_MI-domain was incubated with benzamidine-Sepharose (Amersham Biosciences) to remove thrombin. The α_MI-domain was biotinylated with EZ-link Sulfo-NHS-LC-biotin (Pierce) according to the manufacturer's instructions and dialyzed against TBS. In addition, the α_MI-domain was labeled with ^{125}I using IODO-GEN (Pierce). GST was expressed in *Escherichia coli* using pGEX-4T-1 vector (Amersham Biosciences) and purified by affinity chromatography on glutathione-Sepharose (Amersham Biosciences). Wild-type recombinant human fibrinogen and mutant fibrinogens with progressive truncations in the C-terminal part of their constituent γ-chains, Fg-395 and Fg-390, were prepared as described previously (*13*).

The Fg peptides P2 (γ377−395), P2-C (γ383−395), and their derivatives (Table 1) were synthesized using Fmoc-chemistry. P1 (γ190−202) and H19 (γ340−357) peptides were synthesized as described (*8*). The peptides were purified by RP-HPLC using water/acetonitrile buffer with 0.1% TFA as a mobile phase and analyzed by LC-MS. In addition, the peptide γ273−283, KYRLTYAYFAG, was synthesized. For adhesion assays, all Fg peptides were dissolved in HBSS/HEPES, pH 7.4. γ273−283 was dissolved in dimethyl sulfoxide or 10 mM NaOH and diluted in HBSS/HEPES before being added to cells.

Mab 4A5 against the COOH-terminal end of the fibrinogen γ-chain γ406−411 (*14*) was provided by Dr. G. Matsueda (Bristol-Meyers Squibb). Mab D73H recognizes the fibrinogen Bβ-chain sequence 261−272 (*15*) and was a gift from Dr. P. Simpson-Haidaris (University of Rochester).

Screening of the P2-C Binding Regions Using a P2-C Peptide Array. The overlapping 6-mer peptide library with a one amino acid offset spanning ^{382}TTMKIIPFNRLTIG^{395} was synthesized as spots on cellulose membranes exactly as described (*16*, *17*). The chemical and technical performance of this type of simultaneous parallel solid phase synthesis has been previously optimized and characterized (*18*). Peptides were C-terminally attached to cellulose through a (β-Ala)$_2$ spacer. The membrane-bound library was blocked for 2 h with 1% BSA in TBS and incubated with 10 μg/mL ^{125}I-labeled α_MI-domain in TBS containing 1 mM $MgCl_2$ for 3 h at 22 °C. After washing with TBS+0.05% Tween-20, the membranes were dried and the I-domain binding was visualized by autoradiography.

Expression of Recombinant γC- and βC-Domains and Site-Directed Mutagenesis. The recombinant γC- and βC-domains

were expressed as fusion proteins with GST. The coding regions for the γC-domain (residues Ile^{145}−Val^{411}) and βC-domain (residues Glu^{183}−Gln^{461}) were amplified by polymerase chain reaction using as template plasmids p674 (19) and p668 (*20*), consisting of full-length cDNA encoding the human Fg γ and β chains, respectively. The amplified fragments were cloned in the expression vector pGEX-4T-1 (Amersham Biosciences). The accuracy of the DNA sequence was verified by sequencing. The plasmids were transformed in *E. coli* strain BL-21(DE3)pLysS, and expression was induced by adding 0.6 mM isopropyl-1-thio-β-D-galactopyranoside for 3−4 h at 30 °C. The recombinant proteins were purified from soluble fractions of *E. coli* lysates by affinity chromatography using glutathione-sepharose. Analysis of the purified γC and βC proteins by SDS−PAGE showed major bands migrating as expected (M_r of 60 kD) and minor bands (5−10% in different preparations) of ~30 kD. The intactness of the COOH-terminal end of γC was confirmed by Western blot analysis using mAb 4A5 directed against γ406−411. The expression of βC was monitored by Western blotting using mAb D73H. Both recombinant domains were used as GST fusion proteins to prevent γC and βC aggregation after removal of the fusion part.

Site-directed mutagenesis of the γC-domain was performed by using the QuickChange mutagenesis kit (Stratagene, San Diego, CA). The pGEX-4T-1 construct containing DNA encoding the γC-domain was modified by site-directed mutagenesis using two mutagenic primers containing the desired mutation and the mutant γC-domains were prepared as described above for the recombinant wild-type γC.

Generation of the βC/γC-Domain Chimeras. The segments corresponding to the γC sequences 383−411 and 377−411 were inserted into the homologous positions of the βC domain. To create cDNA for the chimeric βC domains, the following two-step procedure was employed. In the first step, the segment corresponding to the γC carboxyl-terminal sequence Pro^{388}−Val^{411} was inserted after Arg^{455} of the βC-domain. To add γ388−411 to βC, the primer containing the *Stu*I restriction site was used to amplify the γ388−411 encoding segment in the γC-containing plasmid by polymerase chain reaction: 5′-CTATGACGATAAGGCCTTTCAACAGAC-3′ (forward primer; the restriction site is underlined). The reverse primer was pGEX-4T-1 3′ sequencing primer (Amersham Biosciences). To introduce the *Stu*I site into the cDNA fragment encoding βC, the following mutagenic primer was used: 5′-GATGAGGCCTTTCTTCCCACAGCAATAGTC-3′. The PCR fragment and a vector containing mutated βC were digested with *Stu*I and *Not*I (polylinker pGEX-4T-1 site) and ligated using T4 DNA ligase (Promega). The correctness of the insertion was confirmed by sequencing. The plasmid was transformed in *E. coli* strain BL-21(DE3)pLys, and the βC/γC388−411 (designated βC/Ch1) protein was expressed and purified from the cell lysates as a fusion protein with GST under conditions used for the wild-type γC and βC domains. Successful grafting of the γC 388−411 into βC was verified by Western blot analysis using mAb 4A5, which recognizes γC at γ406−411. To generate the chimeric βC/γC382−411 which contains P2-C and βC/γC377−411 which contains the entire P2 sequence, Arg^{448}, Met^{450}, Ser^{451}, and Arg^{455} in βC/Ch1 were substituted with Lys, Thr, Thr, and Ile (corresponding to γ380, γ382, γ383, and γ387), respectively.

Adhesion Assays. Adhesion assays with HEK 293 cells expressing wild-type $\alpha_M\beta_2$ (*21*) were performed essentially as described previously (*22*) using Immulon 4HBX microtiter plates (Dynex Technologies, Chantilly, VA) coated with wild-type and mutant recombinant fibrinogens, or D_{100}, and post-coated with 1% PVP. The $\alpha_M\beta_2$-expressing cells grown in DMEM/F-12 supplemented with 25 mM HEPES and 10% fetal bovine serum were labeled with Calcein AM (Molecular Probes, Eugene, OR) and resuspended in HBSS at 2.5×10^5 cells/mL. The labeled cells (100 μL aliquots) were added to the wells coated with recombinant Fg or preincubated with selected concentrations of peptides for 15 min at 22 °C before being added to the wells coated with D_{100}. After 30 min incubation at 37 °C in 3% CO_2, the nonadherent cells were removed and the fluorescence was measured in a fluorescence plate reader (Applied Biosystems, Farmington, MA). The number of adherent cells was determined from a standard curve constructed using the fluorescence of 100 μL aliquots with a known number of the labeled cells.

Solid-Phase Binding Assays. To test the interaction of the wild-type γC, βC, mutant γC- and chimeric βC/γC-domains with the α_MI-domain, 96-well microtiter plates (Immulon 4HBX, Dynex Technologies Inc., Chantilly, VA) were coated with recombinant Fg domains at 10 μg/mL overnight at 4 °C and post-coated with 1% BSA for 2 h. Different concentrations of the biotinylated α_MI-domain in TBS containing 1 mM $MgCl_2$, 1 mM $CaCl_2$, and 0.05% Tween 20 were added to the wells and incubated for 1 h at 37 °C. After washing, streptavidin conjugated to alkaline phosphatase (Pierce) at 1μg/mL was added and incubated for 30 min at 37 °C. The α_MI-domain binding was detected by reaction with *p*-nitrophenyl phosphate. As a control, the binding of the α_MI-domain to BSA post-coat and 10 μg/mL GST which accounted for ~10% and 20% of that to γC domains, respectively, was subtracted to calculate the specific binding.

Molecular Modeling. Molecular models for the cyclic peptides were constructed by first adding cysteines to both termini of the X-ray coordinates of fibrinogen γ390−395 (PDB identifier 1FZC (*5*)). Molecular dynamic and energy minimization calculations were carried out with the two SH-groups restrained to within 4 Å of each other (InsightII, Accelrys Inc.). This distance restraint was removed and a disulfide bond created before repetition of the dynamics/minimization procedure. Ten different cyclic peptides generated using this procedure were then docked to the α_MI-domain crystal structure (PDB identifier 1IDO) and the resulting complexes subjected to dynamics/minimization calculations.

RESULTS

Mutational Analyses of Recombinant Human Fibrinogen and γC-Domains of Fg. On the basis of studies with synthetic peptides, we have previously proposed that P2, γ377−395, and particularly its γ383−395 portion (P2-C) may represent a major recognition site for $\alpha_M\beta_2$ in the γC-domain of Fg (*8*). Because the removal of γ391−395 resulted in a significant decrease of the inhibitory activity of the synthetic peptide γ377−391 (*8*), the carboxyl-terminal part of P2 was deemed to be critical for its activity. To directly evaluate the role of this part of P2 in $\alpha_M\beta_2$ recognition, we have tested

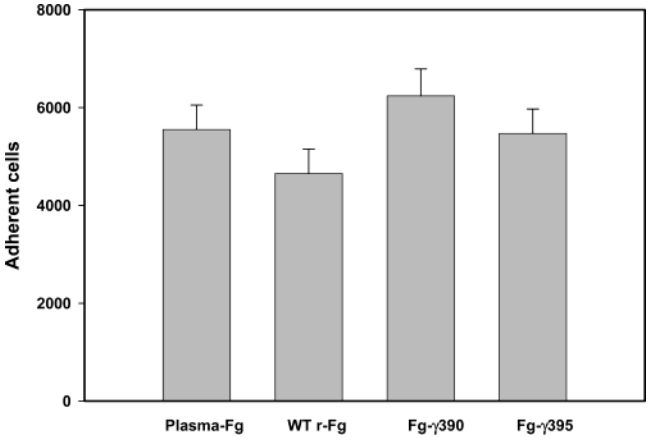

FIGURE 1: Adhesion of the $\alpha_M\beta_2$-expressing cells to recombinant wild-type and mutant Fg. Aliquots (0.1 mL) of Calcein-labeled cells (2.5×10^4) in HBSS supplemented with 1 mM $MgCl_2$ and $CaCl_2$ were added to wells coated with 2.5 μg/mL of recombinant wild-type Fg and mutant Fg-395 and Fg-390. After 30 min incubation at 37 °C in 3% CO_2, the nonadherent cells were removed, and the fluorescence was measured in a fluorescence plate reader. Cell adhesion to 2.5 μg/mL of normal plasma Fg is also shown. The concentration of Fg (2.5 μg/mL) used supports the maximal cells adhesion to each Fg and was determined in the preliminary concentration-dependent analyses. Data are expressed as a percentage of added cells. The values were the average of three separate experiments ± SD.

the capacity of recombinant human Fgs in which either γ395−411 (Fg-395) or γ391−411 (Fg-390) was deleted to support adhesion of the $\alpha_M\beta_2$-expressing HEK 293 cells. As shown in Figure 1, wild-type, mutant Fg-395, and mutant Fg-390 supported similar maximal levels of cell adhesion, suggesting that deletion of γ391−395 in the context of whole Fg is not sufficient to ablate function.

Since recombinant Fg with deletions of the γ-chain beyond Ile^{387} cannot be produced due to defective assembly and secretion (*13*), we have further examined the contribution of the P2 sequence in $\alpha_M\beta_2$ binding by testing the recombinant wild-type γC-domain and a series of γC mutants in which portions of, or the entire P2, were deleted. The wild-type γC and mutants were tested for their ability to interact with the recombinant α_MI-domain. Recent data demonstrated that within $\alpha_M\beta_2$, the I-domain is responsible for Fg binding (*10*). Therefore, the α_MI-domain is able to substitute for the whole receptor in ligand recognition. As shown in Figure 2A, the recombinant α_MI-domain bound to the immobilized γC in a dose-dependent and saturable manner. The binding was inhibited by soluble P2 but not the control peptide H19 (γ340−357) (Figure 2B).

The capacity of γC deletion mutants to bind the α_MI-domain was tested. Removal of the COOH-terminal γ397−411 or γ395−411 segments did not decrease the ability of γC(Δ397−411) and γC(Δ395−411) to bind the α_MI-domain (not shown). Also, mutation of the single residue Arg^{391} in the full-length γC did not alter the activity (not shown). However, sequential truncations of γC resulted in the gradual decline of the binding activities of the γC mutants (Figure 3). Deletion of the γ391−411 segment decreased binding by 26% ± 5% and the subsequent removal of the γ383−411 segment resulted in an additional 25% decline producing a total 50% decrease in the binding activity of γC. Removal of the entire γ377−411 did not decrease the γC activity further. Deletion of 34 residues in the γC($\triangle$377−411)

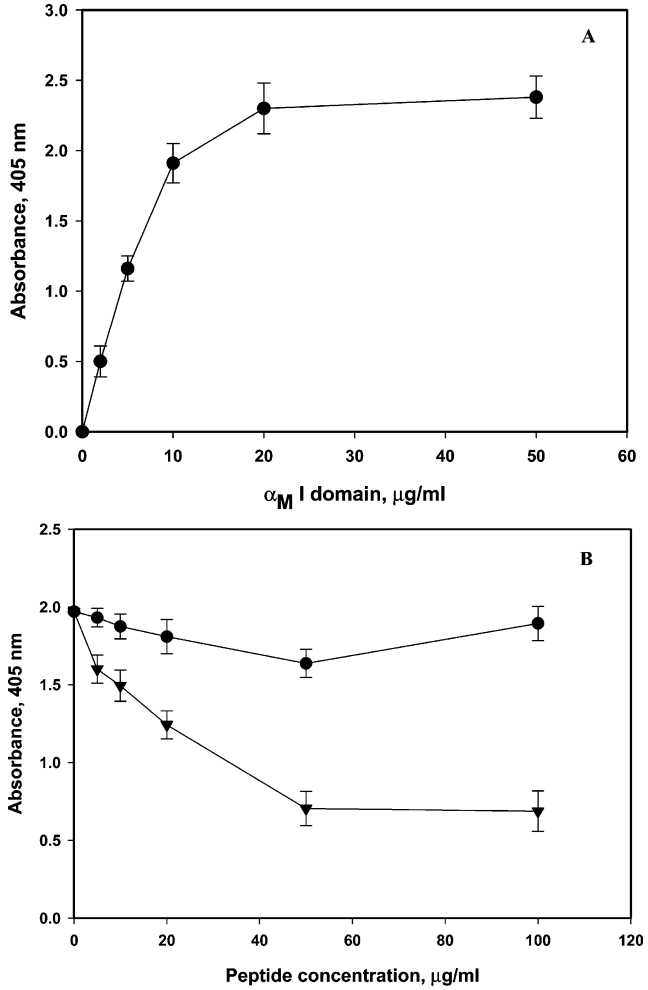

FIGURE 2: Binding of the recombinant α_MI-domain to the recombinant wild-type γC-domain of Fg. Panel A: Different concentrations of biotinylated α_MI-domain in TBS containing 1 mM $MgCl_2$, 1 mM $CaCl_2$, and 0.05% Tween 20 were added to microtiter plates coated with 10 μg/mL of wild-type γC-domain, and post-coated with 1% BSA, then incubated for 1 h at 37 °C. After washing, the bound I-domain was detected using streptavidin conjugated to alkaline-phosphatase with *p*-nitrophenyl phosphate for disclosure. In parallel, nonspecific binding of different α_MI-domain concentrations to 10 μg/mL GST and BSA post-coat was determined (~30%) and was subtracted. Panel B: Binding of 10 μg/mL biotinylated α_MI-domain in the presence of different concentrations of P2 (▼) or H19 (●). Shown in panels A and B are the representative experiments of 3−7 independent determinations performed with triplicates at each experimental point.

mutant, including the γ380−390 segment, which forms the structural β-strand, appears not to be harmful for the functional γC conformation. This is based on the recent data that γC with the γ374−411 segment missing was still appropriately folded (*23*). Thus, removal of P2 led to the significant decrease in the binding activity of γC, suggesting that it is important for α_MI-domain binding. However, γC-($\triangle$383−411) and γC($\triangle$377−411) still retained significant activity, indicating that other γC regions contribute to the interaction with the α_MI-domain. Previous studies have pointed to the P1 sequence, γ190−202, as a second putative binding site in γC for the α_MI-domain (*7*). The role of two residues within P1, Asp^{199} and Gly^{200}, has been tested (*8*), and it was found that substitutions of these residues to Gly−Ala did not decrease the binding activity of γC. In addition to Asp^{199}, the side chains of only three other residues in P1,

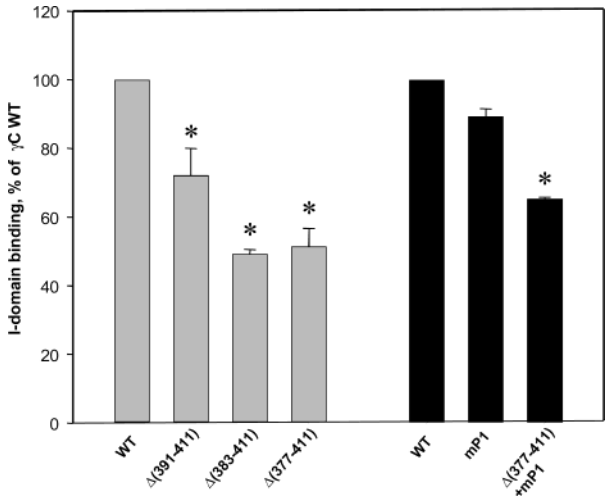

FIGURE 3: Binding of the α_MI-domain to recombinant wild-type γC-domain and γC mutants. The binding of the recombinant α_MI-domain (30 μg/mL) to plates coated with 10 μg/mL of wild-type γC and each γC mutant was determined as described in Figure 2. The concentration of α_MI-domain was determined from the preliminary analyses in which different concentrations of the α_MI-domain were added to 10 μg/mL of recombinant γC domains and is saturating. Nonspecific binding to 10 μg/mL GST+BSA was subtracted. The results are expressed as a percentage of maximal binding attained with the wild-type γC $\pm$ SD. *, statistically different ($p < 0.01$) from the results obtained with wild-type γC. Data for γCΔ(383−411) and γCΔ(377−411) are from 8−10, and for other mutants are from 3−5, independent binding assays, performed in duplicate at each experimental point. mP1 denotes γC mutant in which Lys[196], Arg[197], Leu[198], and Asp[199] in P1 were simultaneously mutated to Ala; γC(Δ377−411) + mP1 is a mutant in which P2 was deleted and four residues in P1 were mutated to Ala.

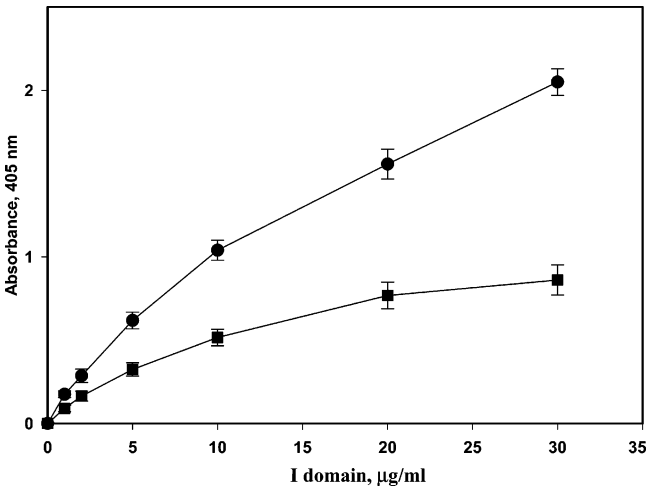

FIGURE 4: The interaction of the α_MI-domain with the wild-type γC- and βC-domains. 10 μg/mL γC (●) and βC (■) domains were immobilized onto the wells of microtiter plates, and the binding of different concentrations of biotinylated α_MI-domain was determined as described in the legend for Figure 1. The result shown was representative of five independent experiments.

Lys[196], Arg[197], and Leu[198] are fully or partially (Arg[197]) exposed on the surface of γC (*5*, *24*) and, therefore, may potentially participate in integrin binding. But the role of these residues, and the combined effect of mutations in P2 and P1 sites on activity of γC, has not been examined. We therefore have generated several γC mutants with substitutions in the P1 sequence alone or in combination with deletions in the P2 region. In these mutants, Lys[196], Arg[197], Leu[198], and Asp[199] were simultaneously substituted with Ala, and the capability of mutant proteins to interact with the α_MI-domain was tested. The binding of γC mutant with quadruple point mutations in P1 was not impaired, and also the introduction of these substitutions in γC($\triangle$377−411) did not decrease the binding activity of the mutant further (Figure 3).

Interaction of the βC-Domain with the α_MI-Domain. The D domain of Fg contains the second subdomain, βC, which is highly homologous to γC, and both γC and βC are folded into almost identical structures (*5*). The major difference between the two domains is the absence in βC of the COOH-terminal segment, homologous to γ390−411. Also, the rest of the sequence homologous to P2-C is poorly conserved. The NH_2-terminal part of P2 is conserved to a higher extent, with only γThr[382] being changed to Met in βC and γThr[383] replaced by Ser. Therefore, we produced recombinant βC and compared its binding to the α_MI-domain with that of γC. As shown in Figure 4, both proteins bound the α_MI-domain. However, the maximal binding of βC was ~2.6-fold lower than that of wild-type γC (37.6±11.4 of γC−WT). These experiments demonstrate the difference between βC and γC in their ability to bind the α_MI-domain and suggest that the P2-C region may be responsible for the higher binding activity of γC.

Inserting of the P2-C Segment into the βC-Domain Improves Binding of Chimera to the α_MI-Domain. To provide direct evidence that P2 contains the binding site for the α_MI-domain, the segment corresponding to P2 was grafted into βC. In the first step of mutagenesis, the γ388−411 segment which contains the C-terminus of P2-C and carboxyl-terminal part of γC was inserted into the homologous position of βC. Then, to restore the entire P2-C and P2 sequences in βC, the Arg[448], Met[450], Ser[451], and Arg[455] in βC were mutated to the corresponding γC residues Lys, Thr, Thr, and Ile, respectively (Figure 5A). The presence of the entire COOH-terminal end of the γ chain in the expressed chimeric proteins was verified with site-specific mAb 4A5 which recognizes the COOH-terminus of γC at γ406−411 (Figure 5B). Inspection of the three-dimensional structures of γC superimposed onto βC (using PDB identifier 1FZC for the DD fragment (*5*)) verified that inserting the P2 sequence into the homologous position of the βC framework was feasible, and that the resulting chimera appears to be appropriately folded. The binding of the α_MI-domain to the chimeric βC/γC-domains is shown in Figure 5C. Inserting the entire P2 sequence into βC improved the binding activity of the chimeric protein by ~2-fold compared to that of the wild-type βC (assessed as maximal binding attained with 30 μg/mL of the biotinylated α_MI-domain). This interaction was blocked by soluble P2, verifying that the α_MI-domain binding to the reconstructed βC-domain was dependent on P2 (not shown). Also, the binding of chimera βC/γC382−411 which incorporated the γ sequence similar to P2-C was examined. This chimera was generated as an intermediate product after grafting γPro[388−411] and mutation of βArg[455], βSer[451], and βMet[450] to γIle, Thr, and Thr, respectively. The binding of this protein was also improved (68.0% $\pm$ 10.4% compared to 37.6% $\pm$ 11.4% for βC-WT). Although the binding of the α_MI-domain to the chimera with inserted P2-C was less than that of the chimera with P2, the difference was not statistically significant.

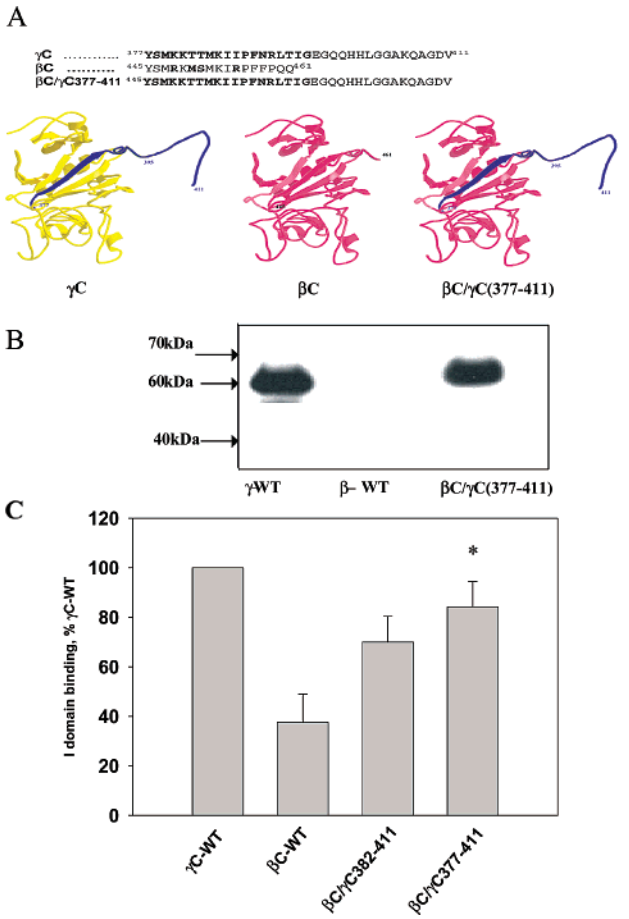

FIGURE 5: Binding of the α_MI-domain to wild-type γC- and βC/γC377−411 chimeric domains. Panel A: Alignment of the γC and βC sequences. The sequence in the engineered βC/γC377−411 chimera is also shown. The human γC 377−395 sequence was aligned with the human βC 445−461 sequence using the NCBI Blast program. The sequence γPro^{388}−Val^{411} was added at the position Pro^{456} of βC to replace βPhe^{457}−Gln^{461} and to produce βC/γC388−411 (chimera βC/Ch-1 generated at the first step). The residues in the βC/Ch-1 chimera, Arg^{448}, Met^{450}, Ser^{451}, and Arg^{455} were replaced with Lys, Thr, Thr, and Ile, corresponding to the γC-domain residues, respectively. Schematic representations of the γC, βC, and the constructed final βC/γC377−411 protein are shown in the bottom. Left, ribbon model of the γC-domain based upon its crystal structure (*24*), PDB identifier 1FIB. Center, ribbon model of the βC-domain, based upon its crystal structure (*5*), PDB identifier 1FZC. Right, schematic drawing of the chimeric domain in which the P2 sequence was placed into the counterpart position of the βC-domain to replace segment β^{445}Tyr−Gln^{461}. Panel B: Western blot analyses of the wild-type γC, βC, and generated chimera βC/γC(377−411). The proteins were electrophoresed on 11% SDS−PAGE gel under reducing conditions, the separated proteins were transferred onto Immobilon P membranes, and the filters were incubated with mAb 4A5 (dilutions 1:1,500) directed against the COOH-terminal end of the γ-chain at 406−411. Bound mAb was detected by reaction with a peroxidase-conjugated second antibody, followed by addition of the 4-chloro-1-naphthol substrate. Positions of the molecular weight markers are shown on the left. Panel C: 30 μg/mL of biotinylated I-domain was added to wild-type γC-, βC- and βC/γC377−411 chimeric domains immobilized on the microtiter plates. The binding of the recombinant α_MI-domain was detected as in Figure 2. The results are expressed as a percentage of maximal binding attained with the wild-type γC ± SD (n = 5). *, statistically different (p < 0.01) from the results obtained with wild-type βC.

Structure Function Analyses of the P2-C Peptide. To define the structural requirements for P2-C activity further, a series of truncated and mutant peptides spanning P2-C were

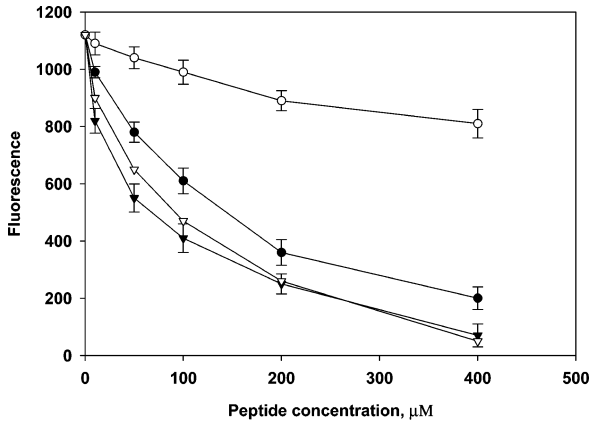

FIGURE 6: Effect of the P2, P2-C, and cyclic NRLTIG peptides on adhesion of the $\alpha_M\beta_2$-expressing cells. $\alpha_M\beta_2$-transfected cells labeled with Calcein AM were incubated with increasing concentrations of P2 (▼), P2-C (▽), and cyclic NRLTIG, nontreated (●) or treated with 2 mM DTT (○), for 15 min at 22 °C. Aliquots (2.5×10^4cells/0.1 mL) were added to the microtiter wells coated with 2 μg/mL the D_{100} fragment and post-coated with 1% PVP. After 30 min at 37 °C, nonadherent cells were removed by three washes with PBS. Results are expressed as fluorescence of adherent cells and are the mean ± SE values from five individual experiments done in triplicate.

synthesized and tested as inhibitors of adhesion of the $\alpha_M\beta_2$-expressing cells (Table 1). To compare the relative inhibitory activity, the IC_{50} values for peptides were determined as described (*8*). In confirmation of previous findings (*8*), the inhibitory potency of P2-C (IC_{50} 42 ± 10 μM) was similar to that of the longer parental peptide P2 (41 ± 8 μM) (Table 1). In addition, the activities of both P2-C variants, a COOH-terminal amide and a COOH-terminal carboxylic acid, were similar. The importance of positively charged residues for the activity of P2-C has been demonstrated by testing peptide P2-CE, in which Lys^{385} and Arg^{391} were substituted with Glu. The inhibitory activity of P2-CE was ~6-fold less (IC_{50} 240±40 μM) than that of parental P2-C. Truncation of five NH_2-terminal residues Thr^{383}− Ile^{387} in γ388−395 resulted in the ~5-fold decrease of the inhibitory activity (180−245 μM). Removal of Pro^{388} and Phe^{389} resulted in yet another drop of activity (IC_{50} 1160 and 1750 for the COOH and NH_2 forms of γ390−395, respectively). Likewise, deletion of the two COOH-terminal residues Ile^{394}-Gly^{395} from γ388−395 caused a ~5-fold decline of γ388−393 activity. Since the activities of γ388−393 (PFNRLT) and γ390−395 (NRLTIG) were similar, it appears that NRLT is the most essential part. To explore the contribution of individual residues in binding function, Arg^{391} in γ390−395 was substituted by Glu. The NELTIG peptide was completely inactive, suggesting that Arg may be important for binding function. The role of Leu within the NRLTIG motif was examined by testing the peptide γ388−395 in which Leu^{392} was substituted with the residue of a similar size, Asp. The mutant peptide was less active than wild-type counterpart as only 35% inhibition was achieved at 2 mM. The inhibitory activity retained by γ390−395 appears to be specific. This was shown in the experiments in which ^{395}NRLTIG^{395} was cyclized through the added flanking cysteines (Figure 6). A 25-fold increase in the inhibitory activity of the cyclic peptide over linear NRLTIG-NH_2 was observed. On the molar basis, the IC_{50} value of cyclic CNRLTIGC (70 ± 20 μM) was only 1.6-fold less than that of P2-C (42 ± 10 μM) (Table 1).

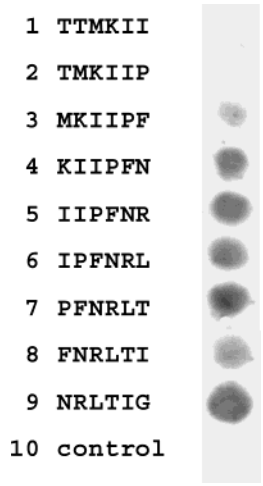

FIGURE 7: The α_MI-domain binding to cellulose-bound peptide scans. The membranes with bound 6-mer peptides derived from P2-C were incubated with 10 μg/mL radioiodinated α_MI-domain for 3 h at 22 °C, washed with TBS+0.05% Tween 20, and bound I-domain was visualized by autoradiography. Spot 10 is the reference spot to define specificity of the α_MI-domain binding to the $(\beta$-Ala$)_2$ spacer. Composition of peptide spots is shown on the right.

Reduction of the cyclic peptide with DTT decreased its inhibitory activity to a level similar to that of the linear peptide (Figure 6). Thus, truncations of P2-C revealed that activity is contained within γ388−395 and that the middle part of γ388−395, NRLT, is the minimal recognition sequence with Arg and Leu being critical residues. In addition, a constrained conformation of NRLTIG is optimal for its anti-adhesive activity. Furthermore, because a significant decrease of activity occurred upon removal of the NH_2-terminal part of P2-C, γ383−389, this region may be essential for the P2-C activity.

To characterize the active regions within P2-C further, we utilized a peptide array consisting of overlapping 6-mer peptides with a one residue shift covering ^{382}TTMKIIPFN-RLTIG^{395} (Figure 7). The membrane with bound peptides was screened for binding of the α_MI-domain. As shown in Figure 7, seven peptides covering the ^{384}Met-Gly^{395} sequence bound the α_MI-domain. No binding to the two NH_2-terminal peptides (spots 1 and 2) was detected. Because the two nonoverlapping peptides, ^{384}MKIIPF^{389} and ^{390}NRLTIG^{395}, can bind the α_MI-domain, P2-C may contain two active regions.

DISCUSSION

In this study, we have examined the role of the γ377−395 sequence in binding of the γC-domain of Fg to the α_MI-domain of $\alpha_M\beta_2$ and analyzed the molecular determinants of the activity of the P2-C peptide which duplicates γ383−395. The major findings of the study are the following: (1) The P2 sequence in γC is directly involved in the α_MI-domain binding since deletion of P2 decreased the binding activity of the γC-domain. Supporting the role of P2 in the α_MI-domain binding, the γC-domain was 2.6-fold more active than the homologous βC-domain. Inserting γ383−395 and γ377−395 into βC imparted the increased binding capacity to the chimeric βC/γC proteins. Finally, multiple point mutations within the P1 sequence did not impair the γC binding function suggesting that γC binding by the α_MI-domain depends on the P2 but not P1 sequence. (2) The NRLTIG sequence within the P2-C peptide represents a minimal recognition motif. This notion is supported by the studies with mutant peptides and by findings that the full anti-adhesive activity of P2-C can be duplicated by cyclic ^{390}NRLTIG^{395} in which Arg and Leu are critical for binding.

Previous studies have demonstrated that the P1, P2, and P2-C peptides inhibited $\alpha_M\beta_2$-mediated cell adhesion and were able to directly support adhesion and to mediate cell migration (*8*, *9*). While the active part of P1 was ascribed to the short sequence γ195−202 (*7*), the minimal motif within P2-C responsible for its activity was not determined. In the present study, we have mapped the active region of P2-C to γ390−395, NRLTIG. The activity of this sequence appears to depend on RL, as evidenced by the data that substitution of Arg^{391} to Glu in NRLTIG resulted in the complete loss of activity and mutation of Leu^{392} resulted in the impaired activity of ^{388}PFNRLTIG^{395}. In addition, this study in combination with previous data (*8*) indicated that the γ384−389 region of P2-C possesses activity. Examination of the two active regions in P2-C, ^{390}N**RL**TIG^{395} and ^{384}M**KI**IPF^{389}, revealed that they contain a similar combination of basic and hydrophobic residues. This can be presented as XBHyX, where B's are positively charged residues R or K, and Hy's are hydrophobic residues are L or I. Hydrophobic residues that flank RL and KI may contribute to activity, and further studies will be required to investigate the contribution of residues in different positions to activity of P2-C. It is noteworthy that P1 peptide also contains RL, and therefore its inhibitory and adhesion-promoting activity may depend on these residues. However, mutations of four residues in P1, including R^{197} and L^{198}, did not decrease the binding function of γC. One potential explanation for the inability of these residues in P1 to function as the binding site for α_MI-domain is that R^{197} is only partially exposed on the surface of γC. This is in contrast to ^{390}NRLTIG^{395} in which all residues are fully exposed in γC.

Although the P2-C peptide was a strong inhibitor of cell adhesion (90% inhibition) and also efficiently blocked the interaction of the D fragment and γC with the recombinant α_MI-domain (*8*), deletion of P2-C from γC resulted in only a 50% decrease of the I-domain binding. Therefore, alternative binding site(s) may participate in the α_MI-domain binding. Because the inhibitory activity of P2-C depends on motifs containing RL, one possibility is that positively charged sequences similar to XRLX in γC may participate in the α_MI-domain binding.

That the ligand recognition by the α_MI-domain might depend on motifs containing the combination of positively charged and hydrophobic residues is supported by the data that P2-C inhibited cell adhesion to the α_EC- and βC-domains of Fg which do not contain the P2-C sequences (*22*). The P2-C peptide and cyclic NRLTIG were also efficient inhibitors of $\alpha_M\beta_2$-mediated cell adhesion to different unrelated $\alpha_M\beta_2$ ligands, including fibronectin, Cy61, thrombospondin, keyhole limpet hemocyanine, thrombin, plasminogen and others (Lishko V., unpublished data, 2002). Inspection of amino acid sequences of γC, α_EC, βC and other tested adhesive proteins revealed that they contain multiple RL(I) or KL(I) motifs or motifs in which Arg or Lys are paired with other hydrophobic residues. For example, γC contains the second RLT motif at the position γ275−277,

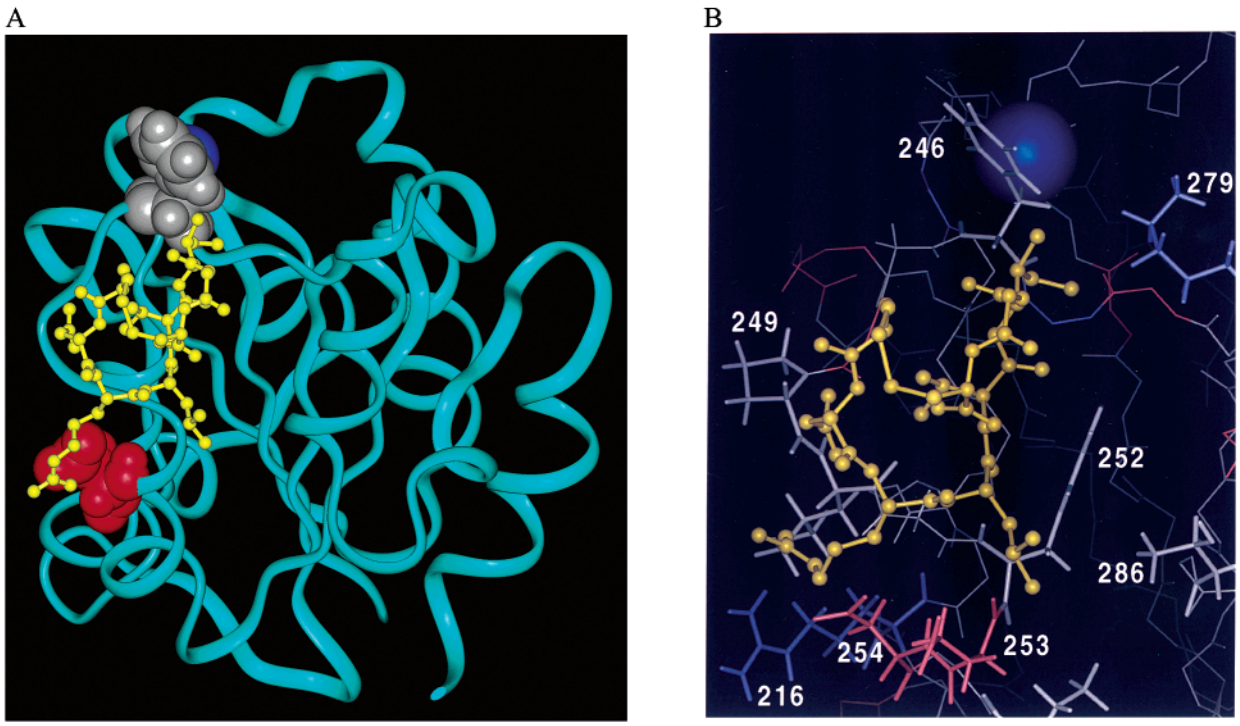

FIGURE 8: Proposed molecular models of cyclic Fg peptide CNRLTIGC bound to the α_MI-domain. Ten molecular models of cyclic CNRLTIGC peptides docked to the α_MI-domain were generated. Initials docking of the peptides to this region was performed by manual rotation and orientation of the peptides until a minimal energy level was obtained. These docked α_MI-domain/peptide complexes were then subjected to dynamic and energy minimization calculations. Panel A: Displayed is a representative model of the cyclic peptide highlighted as yellow ball-and-sticks docked to the α_MI-domain. The ribbon model of the α_MI-domain is based on its crystal structure (PDB identifier 1IDO). The MIDAS cation (blue), Phe^{246}(gray), and Asp^{254}(orange) are displayed as spheres. Phe^{246} and Asp^{254} of the α_MI-domain interact with Ile and Arg of the cyclic peptide, respectively. Panel B: Closeup of the docked peptide. The cyclic peptide is displayed in ball-and-stick fashion in yellow, and the backbone of the α_MI-domain is displayed in stick fashion. The side chains of the α_MI-domain residues that make contact with the cyclic peptide are also displayed and numbered. The cation is shown as a blue sphere.

and the peptide γ^{273}KY**RLT**YAYFAG^{283} blocked $\alpha_M\beta_2$-mediated cell adhesion (IC_{50} 210 ± 30 μM) and supported efficient adhesion (Lishko, V., unpublished data, 2002). Another α_MI-domain ligand, fibronectin (*21*), contains four RL(I)T sequences and five RL(I) pairs. Supporting a critical role of Leu in α_MI-domain recognition, short LLG-based peptides identified by phage display libraries have been found to be efficient inhibitors of α_MI-domain binding to ligands (*25*). Therefore, a likely interpretation of these data is that recognition specificity of Fg and other $\alpha_M\beta_2$ ligands may depend on short linear XRLX or similar motifs. Such limited requirements for ligand recognition by the α_MI-domain seem to fit well with ligand binding promiscuity exhibited by $\alpha_M\beta_2$.

We have demonstrated that within the α_MI-domain the P2-C peptide binds to the Lys^{245}−Arg^{261} segment (*11*) which forms a βD-α5 loop and an adjacent α5 helix and is a unique characteristic of the α_MI-domain (*26*, *27*). In α_MK^{245}−R^{261}, three residues, Phe^{246}, Asp^{254}, and Pro^{257}, have been identified as critical for P2-C binding (*11*). Two of these residues, Phe and Asp, are located at the top of the α_MI-domain in the vicinity of the metal-ion dependent adhesion site, MIDAS (*26*), which has been proposed as a ligand binding interface in the α_MI-domain as well as other I-domains (*28*). In the absence of a crystal structure of the complex and for illustrative purposes, we have generated molecular models of the peptide bound to the α_MI-domain structure. Ten molecular models for the cyclic NRLTIG peptide were constructed and used for docking. Guided by our mutational analysis of the α_MI-domain and by the characterization of the electrostatic and van der Waals surface properties of the α_MI-domain, a site within helix 5 near the MIDAS cation was chosen as the ligand-binding site. One of the most energetically favorable of the 10 structures in shown in Figure 8. In this structure, Arg^{391} of the cyclic peptide forms a salt bridge with α_MAsp^{254} and the peptide's Leu^{392} and Ile^{394}, making hydrophobic interactions with Tyr^{252}/Glu^{253}/Thr^{286} and Lys^{279}/Phe^{246}, respectively. Minimal alterations in the backbone structure of the peptide were observed following binding (0.832 rmsd of superposition of unbound versus bound cyclic peptide), indicating an initial good fit of the cyclic peptide for α_MI-domain. The structure of the bound cyclic peptide was also very similar to its crystal structure, 1FZC (rmsd of 0.824). Limited conformational changes in backbone structure of α_M208−223, 246−253, and 276−288 were noted in most models, with the most perturbed region being nearest the docked peptide, at α_M-254−261.

Previous studies clearly demonstrated the role of acidic residues within ligands for their binding to integrins. In crystal structures of the complexes, an acidic residue from the ligand engages a metal ion at the MIDAS in the integrin I-domain. For example, the aspartic acid of RGDF ligand contacts the βI-domain (*29*) in the crystal of $\alpha_v\beta_3$, while the glutamic acid plays the same role in the complex of collagen peptide with the α_2I-domain of $\alpha_2\beta_1$ (*28*). How, then, does the α_MI-domain bind its ligands? Although the α_MI-domain in the "liganded" conformation was crystallized in the complex with the glutamic acid from the neighboring α_MI-

domain (*26*), which was proposed to play a role of ligand-mimetic, no additional data are available that would imply a role for the acidic residue in $\alpha_M\beta_2$ ligands. The $\alpha_M\beta_2$ binding to its ligands is not RGD inhibitable (*7*), and our data have demonstrated that substitution of positively charged residues for the acidic residue Glu in P2-C decreased the inhibitory activity of the mutant peptide. Thus, it is possible that the ligand engagement by α_MI-domain is achieved by a different mechanism: positively charged and hydrophobic residues participate in receptor docking as demonstrated in this and other studies (*25*, *30*). Alternatively, the α_MI-domain can interact with both XRLX-based peptides and with peptides containing an acidic residue. The precedent for these type of interactions comes from $\alpha_2\beta_1$ which can bind both kinds of peptides (*28*, *30*, *31*). That the two types of interactions are involved in Fg and/or in other $\alpha_M\beta_2$ ligands cannot be presently ruled out. The mechanism by which the α_MI-domain recognizes multiple ligands is speculative but XRLX-based sequences in ligands may be responsible for recognition. We are presently addressing this issue.

ACKNOWLEDGMENT

We thank Dr. Plow for partial support of this work. We thank Dr. G. Matsueda for providing mAb 4A5 and Dr. P. Simpson-Haidaris for mAb D73H. We thank A. Podolnikov for providing a computer program for assembly of peptide scans and Tim Burke for critical reading of the manuscript.

REFERENCES

1. Kishimoto, T. K., Baldwin, E. T., and Anderson, D. C. (1999) *Inflammation: Basic Principles and Clinical Correlates*, 3rd ed., pp 537−569, Lippincott Williams and Wilkins, Philadelphia.
2. Ugarova, T. P., and Yakubenko, V. P. (2001) *Ann. N.Y. Acad. Sci. 936*, 368−386.
3. Lu, H., Smith, C. W., Perrard, J., Bullard, D., Tang, L., Entman, M. L., Beaudet, A. L., and Ballantyne, C. M. (1997) *J. Clin. Invest. 99*, 1340−1350.
4. Altieri, D. C., Agbanyo, F. R., Plescia, J., Ginsberg, M. H., Edgington, T. S., and Plow, E. F. (1990) *J. Biol. Chem. 265*, 12119−12122.
5. Spraggon, G., Everse, S. J., and Doolittle, R. F. (1997) *Nature 389*, 455−462.
6. Medved, L., Litvinovich, S., Ugarova, T., Matsuka, Y., and Ingham, K. (1997) *Biochemistry 36*, 4685−4693.
7. Altieri, D. C., Plescia, J., and Plow, E. F. (1993) *J. Biol. Chem. 268*, 1847−1853.
8. Ugarova, T. P., Solovjov, D. A., Zhang, L., Loukinov, D. I., Yee, V. C., Medved, L. V., and Plow, E. F. (1998) *J. Biol. Chem. 273*, 22519−22527.
9. Forsyth, C. B., Solovjov, D. A., Ugarova, T. P., and Plow, E. F. (2001) *J. Exp. Med. 193*, 1123−1133.
10. Yalamanchili, P., Lu, C. F., Oxvig, C., and Springer, T. A. (2000) *J. Biol. Chem. 275*, 21877−21882.
11. Yakubenko, V. P., Solovjov, D. A., Zhang, L., Yee, V. C., Plow, E. F., and Ugarova, T. P. (2001) *J. Biol. Chem. 275*, 13995−14003.
12. Ugarova, T. P., and Budzynski, A. Z. (1992) *J. Biol. Chem. 267*, 13687−13693.
13. Okumura, N., Terasawa, F., Tanaka, H., Hirota, M., Ota, H., Kitano, K., and Lord, S. T. (2002) *Blood 99*, 3654−3660.
14. Matsueda, G. R., and Bernatowicz, M. S. (1988) in *Fibrinogen 3 − Biochemistry, Biological Functions, Gene Regulation and Expression*, (Mosesson, M. W., Amrani, D., Siebenlist, K. R., and DiOrio, P., Eds.) Elsevier Science Publishers B. V., Amsterdam.
15. Rybarczyk, B. J., Pereira, M., and Simpson-Haidaris, P. J. (2000) *Thromb. Haemostasis 84*, 43−48.
16. Frank, R. (1992) *Tetrahedron 48*, 9217−9232.
17. Kramer, A., and Schneider-Mergener, J. (1998) *Methods Mol. Biol. 89*, 25−39.
18. Frank, R. (2002) *J. Immunol. Methods 267*, 13−26.
19. Bolyard, M. G., and Lord, S. T. (1988) *Gene 66*, 183−192.
20. Bolyard, M. G., and Lord, S. T. (1989) *Blood 73*, 1202−1206.
21. Lishko, V. K., Yakubenko, V. P., and Ugarova, T. P. (2003) *Exp. Cell Res. 283*, 116−126.
22. Lishko, V. K., Yakubenko, V. P., Hertzberg, K. M., Grieninger, G., and Ugarova, T. P. (2001) *Blood 98*, 2448−2455.
23. Yakovlev, S. L. S., Loukinov, D. I., and Medved, L. (2000) *Biochemistry 39*, 15721−15729.
24. Yee, V. C., Pratt, K. P., Cote, H. C. F., LeTrong, I., Chung, D. W., Davie, E. W., Stenkamp, R. E., and Teller, D. C. (1997) *Structure 5*, 125−138.
25. Koivunen, E., Ranta, T. M., Annaila, A., Taube, S., Uppala, A., Jokinen, M., van Willigen, G., and Gahmberg, C. G. (2001) *J. Cell Biol. 153*, 905−915.
26. Lee, J.-O., Rieu, P., Arnaout, M. A., and Liddington, R. (1995) *Cell 80*, 631−638.
27. Lee, J.-O., Bankston, L. A., Arnaout, M. A., and Liddington, R. C. (1995) *Structure 3*, 1333−1340.
28. Emsley, J., Knight, C. G., Farndale, R. W., Barnes, M. J., and Liddington, R. C. (2000) *Cell 101*, 47−56.
29. Xiong, J.-P., Stehle, T., Joachimiak, A., Frech, M., Goodman, S. L., and Arnaout, M. A. (2002) *Science 296*, 151−155.
30. Pentikainen, O., Hoffren, A. M., Ivaska, J., Kapyla, J., Nyronen, T., Heino, J., and Johnson, M. S. (1999) *J. Biol. Chem. 274*, 31495−31505.
31. Ivaska, J., Kapyla, J., Pentikainen, O., Hoffren, A. M., Hermonen, J., Huttunen, P., Johnson, M. S., and Heino, J. (1998) *J. Biol. Chem. 274*, 3513−3521.

BI034057K